

VU Research Portal

Study of the reaction $e^{+}e^{-} \rightarrow J/\psi \pi^{+}\pi^{-}$ via initial-state radiation at BABAR

Lees, J.P.; Raven, H.G.; BARBAR, Collaboration

published in

Physical Review D
2012

DOI (link to publisher)

[10.1103/PhysRevD.86.051102](https://doi.org/10.1103/PhysRevD.86.051102)

document version

Publisher's PDF, also known as Version of record

[Link to publication in VU Research Portal](#)

citation for published version (APA)

Lees, J. P., Raven, H. G., & BARBAR, C. (2012). Study of the reaction $e^{+}e^{-} \rightarrow J/\psi \pi^{+}\pi^{-}$ via initial-state radiation at BABAR. *Physical Review D*, 86(5), [051102]. <https://doi.org/10.1103/PhysRevD.86.051102>

General rights

Copyright and moral rights for the publications made accessible in the public portal are retained by the authors and/or other copyright owners and it is a condition of accessing publications that users recognise and abide by the legal requirements associated with these rights.

- Users may download and print one copy of any publication from the public portal for the purpose of private study or research.
- You may not further distribute the material or use it for any profit-making activity or commercial gain
- You may freely distribute the URL identifying the publication in the public portal ?

Take down policy

If you believe that this document breaches copyright please contact us providing details, and we will remove access to the work immediately and investigate your claim.

E-mail address:

vuresearchportal.ub@vu.nl

Study of the reaction $e^+e^- \rightarrow J/\psi\pi^+\pi^-$ via initial-state radiation at BABAR

J. P. Lees,¹ V. Poireau,¹ V. Tisserand,¹ J. Garra Tico,² E. Grauges,² A. Palano,^{3a,3b} G. Eigen,⁴ B. Stugu,⁴ D. N. Brown,⁵ L. T. Kerth,⁵ Yu. G. Kolomensky,⁵ G. Lynch,⁵ H. Koch,⁶ T. Schroeder,⁶ D. J. Asgeirsson,⁷ C. Hearty,⁷ T. S. Mattison,⁷ J. A. McKenna,⁷ A. Khan,⁸ V. E. Blinov,⁹ A. R. Buzykaev,⁹ V. P. Druzhinin,⁹ V. B. Golubev,⁹ E. A. Kravchenko,⁹ A. P. Onuchin,⁹ S. I. Serednyakov,⁹ Yu. I. Skovpen,⁹ E. P. Solodov,⁹ K. Yu. Todyshev,⁹ A. N. Yushkov,⁹ M. Bondioli,¹⁰ D. Kirkby,¹⁰ A. J. Lankford,¹⁰ M. Mandelkern,¹⁰ H. Atmacan,¹¹ J. W. Gary,¹¹ F. Liu,¹¹ O. Long,¹¹ G. M. Vitug,¹¹ C. Campagnari,¹² T. M. Hong,¹² D. Kovalskyi,¹² J. D. Richman,¹² C. A. West,¹² A. M. Eisner,¹³ J. Kroseberg,¹³ W. S. Lockman,¹³ A. J. Martinez,¹³ B. A. Schumm,¹³ A. Seiden,¹³ D. S. Chao,¹⁴ C. H. Cheng,¹⁴ B. Echenard,¹⁴ K. T. Flood,¹⁴ D. G. Hitlin,¹⁴ P. Ongmongkolkul,¹⁴ F. C. Porter,¹⁴ A. Y. Rakitin,¹⁴ R. Andreassen,¹⁵ Z. Huard,¹⁵ B. T. Meadows,¹⁵ M. D. Sokoloff,¹⁵ L. Sun,¹⁵ P. C. Bloom,¹⁶ W. T. Ford,¹⁶ A. Gaz,¹⁶ U. Nauenberg,¹⁶ J. G. Smith,¹⁶ S. R. Wagner,¹⁶ R. Ayad,^{17,*} W. H. Toki,¹⁷ B. Spaan,¹⁸ K. R. Schubert,¹⁹ R. Schwierz,¹⁹ D. Bernard,²⁰ M. Verderi,²⁰ P. J. Clark,²¹ S. Playfer,²¹ D. Bettoni,^{22a} C. Bozzi,^{22a,22b} R. Calabrese,^{22a,22b} G. Cibinetto,^{22a,22b} E. Fioravanti,^{22a,22b} I. Garzia,^{22a,22b} E. Luppi,^{22a,22b} M. Menerato,^{22a,22b} M. Negrini,^{22a,22b} L. Piemontese,^{22a} V. Santoro,^{22a} R. Baldini-Ferroli,²³ A. Calcaterra,²³ R. de Sangro,²³ G. Finocchiaro,²³ P. Patteri,²³ I. M. Peruzzi,^{23,†} M. Piccolo,²³ M. Rama,²³ A. Zallo,²³ R. Contri,^{24a,24b} E. Guido,^{24a,24b} M. Lo Vetere,^{24a,24b} M. R. Monge,^{24a,24b} S. Passaggio,^{24a} C. Patrignani,^{24a,24b} E. Robutti,^{24a} B. Bhuyan,²⁵ V. Prasad,²⁵ C. L. Lee,²⁶ M. Morii,²⁶ A. J. Edwards,²⁷ A. Adametz,²⁸ U. Uwer,²⁸ H. M. Lacker,²⁹ T. Lueck,²⁹ P. D. Dauncey,³⁰ P. K. Behera,²¹ U. Mallik,³¹ C. Chen,³² J. Cochran,³² W. T. Meyer,³² S. Prell,³² A. E. Rubin,³² A. V. Gritsan,³³ Z. J. Guo,³³ N. Arnaud,³⁴ M. Davier,³⁴ D. Derkach,³⁴ G. Grosdidier,³⁴ F. Le Diberder,³⁴ A. M. Lutz,³⁴ B. Malaescu,³⁴ P. Roudeau,³⁴ M. H. Schune,³⁴ A. Stocchi,³⁴ G. Wormser,³⁴ D. J. Lange,³⁵ D. M. Wright,³⁵ C. A. Chavez,³⁶ J. P. Coleman,³⁶ J. R. Fry,³⁶ E. Gabathuler,³⁶ D. E. Hutchcroft,³⁶ D. J. Payne,³⁶ C. Touramanis,³⁶ A. J. Bevan,³⁷ F. Di Lodovico,³⁷ R. Sacco,³⁷ M. Sigamani,³⁷ G. Cowan,³⁸ D. N. Brown,³⁹ C. L. Davis,³⁹ A. G. Denig,⁴⁰ M. Fritsch,⁴⁰ W. Gradl,⁴⁰ K. Griessinger,⁴⁰ A. Hafner,⁴⁰ E. Prencipe,⁴⁰ R. J. Barlow,^{41,‡} G. Jackson,⁴¹ G. D. Lafferty,⁴¹ E. Behn,⁴² R. Cenci,⁴² B. Hamilton,⁴² A. Jawahery,⁴² D. A. Roberts,⁴² C. Dallapiccola,⁴³ R. Cowan,⁴⁴ D. Dujmic,⁴⁴ G. Sciolla,⁴⁴ R. Cheaib,⁴⁵ D. Lindemann,⁴⁵ P. M. Patel,⁴⁵ S. H. Robertson,⁴⁵ P. Biassoni,^{46a,46b} N. Neri,^{46a} F. Palombo,^{46a,46b} S. Stracka,^{46a,46b} L. Cremaldi,⁴⁷ R. Godang,^{47,§} R. Kroeger,⁴⁷ P. Sonnek,⁴⁷ D. J. Summers,⁴⁷ X. Nguyen,⁴⁸ M. Simard,⁴⁸ P. Taras,⁴⁸ G. De Nardo,^{49a,49b} D. Monorchio,^{49a,49b} G. Onorato,^{49a,49b} C. Sciacca,^{49a,49b} M. Martinelli,⁵⁰ G. Raven,⁵⁰ C. P. Jessop,⁵¹ J. M. LoSecco,⁵¹ W. F. Wang,⁵¹ K. Honscheid,⁵² R. Kass,⁵² J. Brau,⁵³ R. Frey,⁵³ N. B. Sinev,⁵³ D. Strom,⁵³ E. Torrence,⁵³ E. Feltresi,^{54a,54b} N. Gagliardi,^{54a,54b} M. Margoni,^{54a,54b} M. Morandin,^{54a,54b} M. Posocco,^{54a} M. Rotondo,^{54a} G. Simi,^{54a} F. Simonetto,^{54a,54b} R. Stroili,^{54a,54b} S. Akar,⁵⁵ E. Ben-Haim,⁵⁵ M. Bomben,⁵⁵ G. R. Bonneaud,⁵⁵ H. Briand,⁵⁵ G. Calderini,⁵⁵ J. Chauveau,⁵⁵ O. Hamon,⁵⁵ Ph. Leruste,⁵⁵ G. Marchiori,⁵⁵ J. Ocariz,⁵⁵ S. Sitt,⁵⁵ M. Biasini,^{a56a,56b} E. Manoni,^{a56a,56b} S. Pacetti,^{a56a,56b} A. Rossi,^{a56a,56b} C. Angelini,^{57a,57b} G. Batignani,^{57a,57b} S. Bettarini,^{57a,57b} M. Carpinelli,^{57a,57b,||} G. Casarosa,^{57a,57b} A. Cervelli,^{57a,57b} F. Forti,^{57a,57b} M. A. Giorgi,^{57a,57b} A. Lusiani,^{57a,57c} B. Oberhof,^{57a,57b} E. Paoloni,^{57a,57b} A. Perez,^{57a} G. Rizzo,^{57a,57b} J. J. Walsh,^{57a} D. Lopes Pegna,⁵⁸ J. Olsen,⁵⁸ A. J. S. Smith,⁵⁸ A. V. Telnov,⁵⁸ F. Anulli,^{59a} R. Faccini,^{59a,59b} F. Ferrarotto,^{59a} F. Ferroni,^{59a,59b} M. Gaspero,^{59a,59b} L. Li Gioi,^{59a} M. A. Mazzoni,^{59a} G. Piredda,^{59a} C. Büniger,⁶⁰ O. Grünberg,⁶⁰ T. Hartmann,⁶⁰ T. Leddig,⁶⁰ H. Schröder,⁶⁰ C. Voss,⁶⁰ R. Waldi,⁶⁰ T. Adye,⁶¹ E. O. Olaiya,⁶¹ F. F. Wilson,⁶¹ S. Emery,⁶² G. Hamel de Monchenault,⁶² G. Vasseur,⁶² Ch. Yèche,⁶² D. Aston,⁶³ D. J. Bard,⁶³ R. Bartoldus,⁶³ J. F. Benitez,⁶³ C. Cartaro,⁶³ M. R. Convery,⁶³ J. Dorfan,⁶³ G. P. Dubois-Felsmann,⁶³ W. Dunwoodie,⁶³ M. Ebert,⁶³ R. C. Field,⁶³ M. Franco Sevilla,⁶³ B. G. Fulsom,⁶³ A. M. Gabareen,⁶³ M. T. Graham,⁶³ P. Grenier,⁶³ C. Hast,⁶³ W. R. Innes,⁶³ M. H. Kelsey,⁶³ P. Kim,⁶³ M. L. Kocian,⁶³ D. W. G. S. Leith,⁶³ P. Lewis,⁶³ B. Lindquist,⁶³ S. Luitz,⁶³ V. Luth,⁶³ H. L. Lynch,⁶³ D. B. MacFarlane,⁶³ D. R. Muller,⁶³ H. Neal,⁶³ S. Nelson,⁶³ M. Perl,⁶³ T. Pulliam,⁶³ B. N. Ratcliff,⁶³ A. Roodman,⁶³ A. A. Salnikov,⁶³ R. H. Schindler,⁶³ A. Snyder,⁶³ D. Su,⁶³ M. K. Sullivan,⁶³ J. Va'vra,⁶³ A. P. Wagner,⁶³ W. J. Wisniewski,⁶³ M. Wittgen,⁶³ D. H. Wright,⁶³ H. W. Wulsin,⁶³ C. C. Young,⁶³ V. Ziegler,⁶³ W. Park,⁶⁴ M. V. Purohit,⁶⁴ R. M. White,⁶⁴ J. R. Wilson,⁶⁴ A. Randle-Conde,⁶⁵ S. J. Sekula,⁶⁵ M. Bellis,⁶⁶ P. R. Burchat,⁶⁶ T. S. Miyashita,⁶⁶ M. S. Alam,⁶⁷ J. A. Ernst,⁶⁷ R. Gorodeisky,⁶⁸ N. Guttman,⁶⁸ D. R. Peimer,⁶⁸ A. Soffer,⁶⁸ P. Lund,⁶⁹ S. M. Spanier,⁶⁹ J. L. Ritchie,⁷⁰ A. M. Ruland,⁷⁰ R. F. Schwitters,⁷⁰ B. C. Wray,⁷⁰ J. M. Izen,⁷¹ X. C. Lou,⁷¹ F. Bianchi,^{72a,72b} D. Gamba,^{72a,72b} L. Lanceri,^{73a,73b} L. Vitale,^{73a,73b} F. Martinez-Vidal,⁷⁴ A. Oyanguren,⁷⁴ H. Ahmed,⁷⁵ J. Albert,⁷⁵ Sw. Banerjee,⁷⁵ F. U. Bernlochner,⁷⁵ H. H. F. Choi,⁷⁵ G. J. King,⁷⁵ R. Kowalewski,⁷⁵ M. J. Lewczuk,⁷⁵ I. M. Nugent,⁷⁵ J. M. Roney,⁷⁵ R. J. Sobie,⁷⁵

N. Tasneem,⁷⁵ T. J. Gershon,⁷⁶ P. F. Harrison,⁷⁶ T. E. Latham,⁷⁶ E. M. T. Puccio,⁷⁶ H. R. Band,⁷⁷ S. Dasu,⁷⁷ Y. Pan,⁷⁷
R. Prepost,⁷⁷ and S. L. Wu⁷⁷

(BABAR Collaboration)

- ¹*Laboratoire d'Annecy-le-Vieux de Physique des Particules (LAPP), Université de Savoie, CNRS/IN2P3, F-74941 Annecy-Le-Vieux, France*
- ²*Universitat de Barcelona, Facultat de Física, Departament ECM, E-08028 Barcelona, Spain*
- ^{3a}*INFN Sezione di Bari, I-70126 Bari, Italy*
- ^{3b}*Dipartimento di Fisica, Università di Bari, I-70126 Bari, Italy*
- ⁴*University of Bergen, Institute of Physics, N-5007 Bergen, Norway*
- ⁵*Lawrence Berkeley National Laboratory and University of California, Berkeley, California 94720, USA*
- ⁶*Ruhr Universität Bochum, Institut für Experimentalphysik I, D-44780 Bochum, Germany*
- ⁷*University of British Columbia, Vancouver, British Columbia, Canada V6T 1Z1*
- ⁸*Brunel University, Uxbridge, Middlesex UB8 3PH, United Kingdom*
- ⁹*Budker Institute of Nuclear Physics, Novosibirsk 630090, Russia*
- ¹⁰*University of California at Irvine, Irvine, California 92697, USA*
- ¹¹*University of California at Riverside, Riverside, California 92521, USA*
- ¹²*University of California at Santa Barbara, Santa Barbara, California 93106, USA*
- ¹³*University of California at Santa Cruz, Institute for Particle Physics, Santa Cruz, California 95064, USA*
- ¹⁴*California Institute of Technology, Pasadena, California 91125, USA*
- ¹⁵*University of Cincinnati, Cincinnati, Ohio 45221, USA*
- ¹⁶*University of Colorado, Boulder, Colorado 80309, USA*
- ¹⁷*Colorado State University, Fort Collins, Colorado 80523, USA*
- ¹⁸*Technische Universität Dortmund, Fakultät Physik, D-44221 Dortmund, Germany*
- ¹⁹*Technische Universität Dresden, Institut für Kern- und Teilchenphysik, D-01062 Dresden, Germany*
- ²⁰*Laboratoire Leprince-Ringuet, Ecole Polytechnique, CNRS/IN2P3, F-91128 Palaiseau, France*
- ²¹*University of Edinburgh, Edinburgh EH9 3JZ, United Kingdom*
- ^{22a}*INFN Sezione di Ferrara, I-44100 Ferrara, Italy*
- ^{22b}*Dipartimento di Fisica, Università di Ferrara, I-44100 Ferrara, Italy*
- ²³*INFN Laboratori Nazionali di Frascati, I-00044 Frascati, Italy*
- ^{24a}*INFN Sezione di Genova, I-16146 Genova, Italy*
- ^{24b}*Dipartimento di Fisica, Università di Genova, I-16146 Genova, Italy*
- ²⁵*Indian Institute of Technology Guwahati, Guwahati, Assam, 781 039, India*
- ²⁶*Harvard University, Cambridge, Massachusetts 02138, USA*
- ²⁷*Harvey Mudd College, Claremont, California 91711*
- ²⁸*Universität Heidelberg, Physikalisches Institut, Philosophenweg 12, D-69120 Heidelberg, Germany*
- ²⁹*Humboldt-Universität zu Berlin, Institut für Physik, Newtonstr. 15, D-12489 Berlin, Germany*
- ³⁰*Imperial College London, London, SW7 2AZ, United Kingdom*
- ³¹*University of Iowa, Iowa City, Iowa 52242, USA*
- ³²*Iowa State University, Ames, Iowa 50011-3160, USA*
- ³³*Johns Hopkins University, Baltimore, Maryland 21218, USA*
- ³⁴*Laboratoire de l'Accélérateur Linéaire, IN2P3/CNRS et Université Paris-Sud 11, Centre Scientifique d'Orsay, B. P. 34, F-91898 Orsay Cedex, France*
- ³⁵*Lawrence Livermore National Laboratory, Livermore, California 94550, USA*
- ³⁶*University of Liverpool, Liverpool L69 7ZE, United Kingdom*
- ³⁷*Queen Mary, University of London, London, E1 4NS, United Kingdom*
- ³⁸*University of London, Royal Holloway and Bedford New College, Egham, Surrey TW20 0EX, United Kingdom*
- ³⁹*University of Louisville, Louisville, Kentucky 40292, USA*
- ⁴⁰*Johannes Gutenberg-Universität Mainz, Institut für Kernphysik, D-55099 Mainz, Germany*
- ⁴¹*University of Manchester, Manchester M13 9PL, United Kingdom*
- ⁴²*University of Maryland, College Park, Maryland 20742, USA*
- ⁴³*University of Massachusetts, Amherst, Massachusetts 01003, USA*
- ⁴⁴*Massachusetts Institute of Technology, Laboratory for Nuclear Science, Cambridge, Massachusetts 02139, USA*
- ⁴⁵*McGill University, Montréal, Québec, Canada H3A 2T8*
- ^{46a}*INFN Sezione di Milano, I-20133 Milano, Italy*
- ^{46b}*Dipartimento di Fisica, Università di Milano, I-20133 Milano, Italy*
- ⁴⁷*University of Mississippi, University, Mississippi 38677, USA*
- ⁴⁸*Université de Montréal, Physique des Particules, Montréal, Québec, Canada H3C 3J7*
- ^{49a}*INFN Sezione di Napoli, I-80126 Napoli, Italy*

^{49b}*Dipartimento di Scienze Fisiche, Università di Napoli Federico II, I-80126 Napoli, Italy*

⁵⁰*NIKHEF, National Institute for Nuclear Physics and High Energy Physics, NL-1009 DB Amsterdam, The Netherlands*

⁵¹*University of Notre Dame, Notre Dame, Indiana 46556, USA*

⁵²*Ohio State University, Columbus, Ohio 43210, USA*

⁵³*University of Oregon, Eugene, Oregon 97403, USA*

^{54a}*INFN Sezione di Padova, I-35131 Padova, Italy*

^{54b}*Dipartimento di Fisica, Università di Padova, I-35131 Padova, Italy*

⁵⁵*Laboratoire de Physique Nucléaire et de Hautes Energies, IN2P3/CNRS, Université Pierre et Marie Curie-Paris6,*

Université Denis Diderot-Paris7, F-75252 Paris, France

^{56a}*INFN Sezione di Perugia, I-06100 Perugia, Italy*

^{56b}*Dipartimento di Fisica, Università di Perugia, I-06100 Perugia, Italy*

^{57a}*INFN Sezione di Pisa, I-56127 Pisa, Italy*

^{57b}*Dipartimento di Fisica, Università di Pisa, I-56127 Pisa, Italy*

^{57c}*Scuola Normale Superiore di Pisa, I-56127 Pisa, Italy*

⁵⁸*Princeton University, Princeton, New Jersey 08544, USA*

^{59a}*INFN Sezione di Roma, I-00185 Roma, Italy*

^{59b}*Dipartimento di Fisica, Università di Roma La Sapienza, I-00185 Roma, Italy*

⁶⁰*Universität Rostock, D-18051 Rostock, Germany*

⁶¹*Rutherford Appleton Laboratory, Chilton, Didcot, Oxon, OX11 0QX, United Kingdom*

⁶²*CEA, Irfu, SPP, Centre de Saclay, F-91191 Gif-sur-Yvette, France*

⁶³*SLAC National Accelerator Laboratory, Stanford, California 94309 USA*

⁶⁴*University of South Carolina, Columbia, South Carolina 29208, USA*

⁶⁵*Southern Methodist University, Dallas, Texas 75275, USA*

⁶⁶*Stanford University, Stanford, California 94305-4060, USA*

⁶⁷*State University of New York, Albany, New York 12222, USA*

⁶⁸*Tel Aviv University, School of Physics and Astronomy, Tel Aviv, 69978, Israel*

⁶⁹*University of Tennessee, Knoxville, Tennessee 37996, USA*

⁷⁰*University of Texas at Austin, Austin, Texas 78712, USA*

⁷¹*University of Texas at Dallas, Richardson, Texas 75083, USA*

^{72a}*INFN Sezione di Torino, I-10125 Torino, Italy*

^{72b}*Dipartimento di Fisica Sperimentale, Università di Torino, I-10125 Torino, Italy*

^{73a}*INFN Sezione di Trieste, I-34127 Trieste, Italy*

^{73b}*Dipartimento di Fisica, Università di Trieste, I-34127 Trieste, Italy*

⁷⁴*IFIC, Universitat de Valencia-CSIC, E-46071 Valencia, Spain*

⁷⁵*University of Victoria, Victoria, British Columbia, Canada V8W 3P6*

⁷⁶*Department of Physics, University of Warwick, Coventry CV4 7AL, United Kingdom*

⁷⁷*University of Wisconsin, Madison, Wisconsin 53706, USA*

(Received 11 April 2012; published 12 September 2012)

We study the process $e^+e^- \rightarrow J/\psi \pi^+ \pi^-$ with initial-state-radiation events produced at the PEP-II asymmetric-energy collider. The data were recorded with the *BABAR* detector at center-of-mass energies 10.58 and 10.54 GeV, and correspond to an integrated luminosity of 454 fb^{-1} . We investigate the $J/\psi \pi^+ \pi^-$ mass distribution in the region from 3.5 to 5.5 GeV/c^2 . Below 3.7 GeV/c^2 the $\psi(2S)$ signal dominates, and above 4 GeV/c^2 there is a significant peak due to the $Y(4260)$. A fit to the data in the range 3.74–5.50 GeV/c^2 yields a mass value $4245 \pm 5(\text{stat}) \pm 4(\text{syst}) \text{ MeV}/c^2$ and a width value $114_{-15}^{+16}(\text{stat}) \pm 7(\text{syst}) \text{ MeV}$ for this state. We do not confirm the report from the Belle Collaboration of a broad structure at 4.01 GeV/c^2 . In addition, we investigate the $\pi^+ \pi^-$ system which results from $Y(4260)$ decay.

DOI: [10.1103/PhysRevD.86.051102](https://doi.org/10.1103/PhysRevD.86.051102)

PACS numbers: 13.20.Gd, 13.25.Gv, 13.66.Bc, 14.40.Pq

*Now at the University of Tabuk, Tabuk 71491, Saudi Arabia.

†Also with Università di Perugia, Dipartimento di Fisica, Perugia, Italy.

‡Now at the University of Huddersfield, Huddersfield HD1 3DH, United Kingdom.

§Now at University of South Alabama, Mobile, Alabama 36688, USA.

||Also with Università di Sassari, Sassari, Italy.

The observation of the $X(3872)$ [1], followed by the discovery of other states such as the $\chi_{c2}(2P)(3930)$ [2], the $Y(3940)$ [3], and the $X(3940)$ [4], has reopened interest in charmonium spectroscopy. These resonances cannot be fully explained by a simple charmonium model [5]. The $Y(4260)$ was discovered [6] in the initial-state-radiation (ISR) process $e^+e^- \rightarrow \gamma_{\text{ISR}} Y(4260)$, $Y(4260) \rightarrow J/\psi \pi^+ \pi^-$. Since it is produced directly in e^+e^- annihilation, it has $J^{PC} = 1^{--}$. The observation of the decay

mode $J/\psi \pi^0 \pi^0$ [7] established that it has zero isospin. However it is not observed to decay to $D^* \bar{D}^*$ [8], nor to $D_s^* \bar{D}_s^*$ [9], so that its properties do not lend themselves to a simple charmonium interpretation, and its nature is still unclear. Other interpretations, such as a four-quark state [10,11], a baryonium state [12], or a hybrid state [13], have been proposed. However if the $Y(4260)$ is a four-quark state it is expected to decay to $D_s^+ \bar{D}_s^-$ [11], but this has not been observed [9].

An analysis of the reaction $e^+e^- \rightarrow J/\psi \pi^+ \pi^-$ [14] which confirms the $Y(4260)$, suggests the existence of a broad state with mass $m = 4008 \pm 40_{-28}^{+114}$ MeV/ c^2 and width $\Gamma = 226 \pm 44 \pm 87$ MeV. Two additional $J^{PC} = 1^{--}$ states, the $Y(4360)$ and the $Y(4660)$, have been reported in ISR production, but only in the reaction $e^+e^- \rightarrow \psi(2S) \pi^+ \pi^-$ [15,16].

In this paper we present an ISR study of the reaction $e^+e^- \rightarrow J/\psi \pi^+ \pi^-$ in the center-of-mass (c.m.) energy (Ecm) range 3.5–5.5 GeV. In the $J/\psi \pi^+ \pi^-$ mass region below ~ 3.7 GeV/ c^2 the signal due to the decay $\psi(2S) \rightarrow J/\psi \pi^+ \pi^-$ dominates. A detailed comparison to $\psi(2S)$ Monte Carlo (MC) simulation yields values of the cross section and partial width to e^+e^- . The high-mass tail of the $\psi(2S)$ MC distribution describes the data up to ~ 4 GeV/ c^2 quite well, and so we perform a maximum likelihood fit over the 3.74–5.50 GeV/ c^2 mass region in which the fit function consists of the incoherent superposition of a nonresonant, decreasing exponential function describing the $J/\psi \pi^+ \pi^-$ mass region above 3.74 GeV/ c^2 and a Breit-Wigner (BW) function describing production and decay of the $Y(4260)$. Non- J/ψ background is treated by means of a simultaneous fit to the mass distribution from the J/ψ sideband regions.

This analysis uses a data sample corresponding to an integrated luminosity of 454 fb $^{-1}$, recorded by the *BABAR* detector at the SLAC PEP-II asymmetric-energy e^+e^- collider operating at c.m. energies 10.58 and 10.54 GeV. The detector is described in detail elsewhere [17]. Charged-particle momenta are measured with a tracking system consisting of a five-layer, double-sided silicon vertex tracker (SVT), and a 40-layer drift chamber (DCH), both of which are coaxial with the 1.5-T magnetic field of a superconducting solenoid. An internally reflecting ring-imaging Cherenkov detector, and specific ionization measurements from the SVT and DCH, provide charged-particle identification (PID). A CsI(Tl) electromagnetic calorimeter (EMC) is used to detect and identify photons and electrons, and muons are identified using information from the instrumented flux-return system.

We reconstruct events corresponding to the reaction $e^+e^- \rightarrow \gamma_{\text{ISR}} J/\psi \pi^+ \pi^-$, where γ_{ISR} represents a photon that is radiated from the initial state e^\pm , thus lowering the c.m. energy of the e^+e^- collision which produces the $J/\psi \pi^+ \pi^-$ system. We do not require observation of the ISR photon, since it is detectable in the EMC for only

$\sim 15\%$ of the events. This is because the ISR photon is produced predominantly in a direction close to the e^+e^- collision axis, and as such is most frequently outside the fiducial region of the EMC.

We select events containing exactly four charged-particle tracks, and reconstruct J/ψ candidates via their decay to e^+e^- or $\mu^+\mu^-$. For each mode, at least one of the leptons must be identified on the basis of PID information. When possible, electron candidates are combined with associated photons in order to recover bremsstrahlung energy loss, and so improve the J/ψ momentum measurement. An e^+e^- ($\mu^+\mu^-$) pair with invariant mass within $(-75, +55)$ MeV/ c^2 ($(-55, +55)$ MeV/ c^2) of the nominal J/ψ mass [18] is accepted as a J/ψ candidate. We refer to the combination of these e^+e^- and $\mu^+\mu^-$ mass intervals as “the J/ψ signal region”. Each J/ψ candidate is subjected to a geometric fit in which the decay vertex is constrained to the e^+e^- interaction region. The χ^2 probability of this fit must be greater than 0.001. An accepted J/ψ candidate is kinematically constrained to the nominal J/ψ mass [18] and combined with a candidate $\pi^+ \pi^-$ pair in a geometric fit which must yield a vertex- χ^2 probability greater than 0.001. At least one pion must be well-identified by using PID information, and neither can satisfy our electron identification criteria.

The value of the missing-mass-squared recoiling against the $J/\psi \pi^+ \pi^-$ system must be in the range $(-0.50, +0.75)$ (GeV/ c^2) 2 in order to be consistent with the recoil of an ISR photon. We require also that the transverse component of the missing momentum be less than 2.25 GeV/ c . If the ISR photon is detected in the EMC, its momentum vector is added to that of the $J/\psi \pi^+ \pi^-$ system in calculating the missing momentum. The candidate $\pi^+ \pi^-$ system has a small residual contamination due to e^+e^- pairs from photon conversions. We compute the pair mass $m_{e^+e^-}$ with the electron mass assigned to each candidate pion, and remove events with $m_{e^+e^-} < 50$ MeV/ c^2 . We estimate the remaining background by using events that have an e^+e^- ($\mu^+\mu^-$) mass in the J/ψ sideband (2.896, 2.971) or (3.201, 3.256) ((2.936, 2.991) or (3.201, 3.256)) GeV/ c^2 after satisfying the other signal region selection criteria.

The $J/\psi \pi^+ \pi^-$ invariant-mass distribution in the region below 4 GeV/ c^2 is dominated by the $\psi(2S)$ signal. The peak region, after subtraction of background from the J/ψ sideband regions, is shown in Fig. 1(a) (solid dots). The open dots indicate the $\psi(2S)$ MC distribution, modified as described below. The data distribution above ~ 3.75 GeV/ c^2 [Fig. 1(b)] may be due to the $\psi(2S)$ tail and a possible $J/\psi \pi^+ \pi^-$ continuum (i.e. nonresonant) contribution. In order to investigate this we performed a detailed comparison of the $\psi(2S)$ signal in data and in MC simulation. For the latter, we used the MC generator VECTORISR [19] and a simulation of the *BABAR* detector based on Geant4 [20]. The resulting MC events were

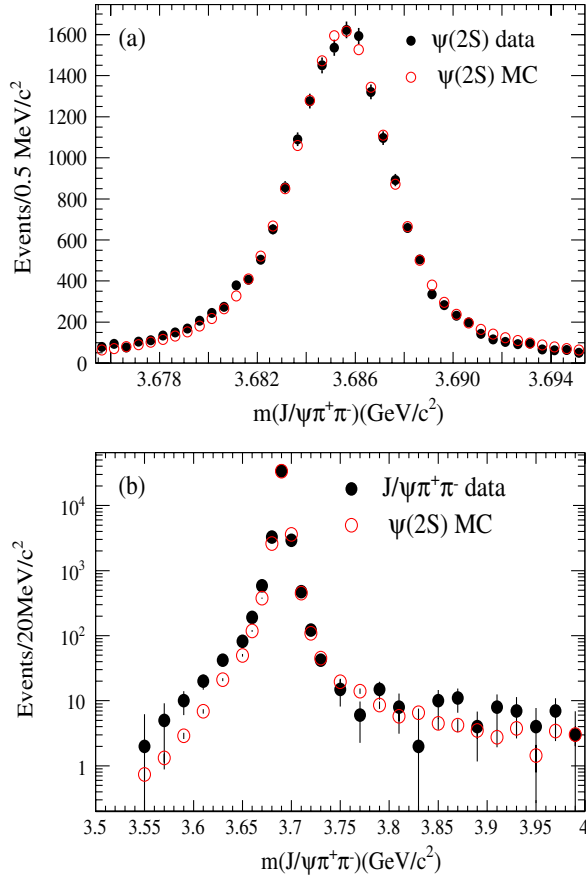


FIG. 1 (color online). (a) The background-subtracted data, and MC simulation modified as described in the text, for the $\psi(2S)$ peak region. (b) The corresponding distribution for the mass region below $4.0 \text{ GeV}/c^2$.

subjected to the reconstruction procedures which were applied to the data.

We first measured the peak mass position for both distributions. We performed a χ^2 -fit of a parabola to the data and MC distributions in intervals of $0.5 \text{ MeV}/c^2$ for the region within $\pm 5 \text{ MeV}/c^2$ of the nominal $\psi(2S)$ mass [18]. For the data, this gave a peak mass value of $3685.32 \pm 0.02(\text{stat}) \text{ MeV}/c^2$, which is $0.77 \pm 0.04 \text{ MeV}/c^2$ less than the nominal value [18]. For the MC events, the result was $3685.43 \pm 0.01(\text{stat}) \text{ MeV}/c^2$, which is $0.66 \pm 0.01 \text{ MeV}/c^2$ smaller than the input value [18]. These deviations are attributed to final-state-radiation effects. The larger deviation obtained for data may result from underestimated energy-loss corrections, and/or magnetic field uncertainty [21,22]. Each MC event was then displaced by $0.11 \text{ MeV}/c^2$ toward lower mass, and the parabolic fit to the new MC distribution was repeated. The MC distribution was normalized to the data by using the data-to-MC ratio of the maxima of the fitted functions. In order to improve the MC-data resolution agreement, a χ^2 function incorporating the data-MC histogram differences and their uncertainties was created for the region within $\pm 10 \text{ MeV}/c^2$ of the peak mass value. In the minimization

procedure each MC event was represented in mass by a superposition of two Gaussian functions with a common center, but different fractional contributions, and normalized to one event. The root-mean-squared (r.m.s.) deviations of the Gaussian functions, and the fractional contribution of the narrower Gaussian function to the normalized distribution, were allowed to vary in the fit, and the contribution of each smeared MC event to each histogram interval was accumulated. This procedure yielded a new MC histogram to be used in the fit to the data histogram. We iterated the above procedure until the change in χ^2 was less than 0.1, at which point the narrow (broad) Gaussian r.m.s. deviation was $0.7(6.3) \text{ MeV}/c^2$, and the fractional contribution was $0.88(0.12)$.

In Fig. 1(a) the final MC distribution is compared to the data in the fit region, and the agreement is good ($\chi^2/\text{NDF} = 30.7/35$, probability = 67.6%; NDF is the number of degrees of freedom). We integrate this MC distribution over the entire lineshape in order to estimate the $\psi(2S)$ signal yield in data, and obtain $20893 \pm 145(\text{stat})$ events. We use the efficiency and the distributed luminosity (obtained from the nominal integrated luminosity and the second-order radiator function from Ref. [23]) to obtain the cross section value $14.05 \pm 0.26(\text{stat}) \text{ pb}$ for radiative return to the $\psi(2S)$. This is in agreement with a previous measurement [14]. In addition we extract $\Gamma(\psi(2S) \rightarrow e^+e^-) = 2.31 \pm 0.05(\text{stat}) \text{ keV}$, in excellent agreement with Ref. [18].

In Fig. 1(b) we compare the modified $\psi(2S)$ MC distribution to the data in the region below $4.0 \text{ GeV}/c^2$. The MC low-mass tail is systematically below the data distribution, but the high-mass tail provides a good description of the observed events. However, we note that the extrapolation to this region requires the use of the $\psi(2S)$ Breit-Wigner lineshape at mass values which are as much as 1000 full-widths beyond the central mass. The existence of many other measured final state contributions to the $J^{PC} = 1^{--}$ amplitude in this mass region must call this procedure into question. Although our model adequately describes the data between the $\psi(2S)$ peak and $\sim 4.0 \text{ GeV}/c^2$, we cannot discount the possibility of a contribution from an $e^+e^- \rightarrow J/\psi \pi^+ \pi^-$ continuum cross section in this region. In this regard, the failure of the MC lineshape to describe the data in the region of the low-mass tail might be due to the threshold rise of just such a continuum cross section.

The $J/\psi \pi^+ \pi^-$ mass distribution corresponding to the J/ψ signal region is shown from 3.74 to $5.5 \text{ GeV}/c^2$ in Fig. 2(a). The shaded histogram, which has been obtained by linear interpolation from the J/ψ sideband regions, represents the estimated background contribution to the J/ψ signal region. The signal distribution shows an excess of events over background above $3.74 \text{ GeV}/c^2$ which might result from the $\psi(2S)$ tail and a possible $J/\psi \pi^+ \pi^-$ continuum contribution, as discussed with respect to Fig. 1(b). At higher mass we observe clear

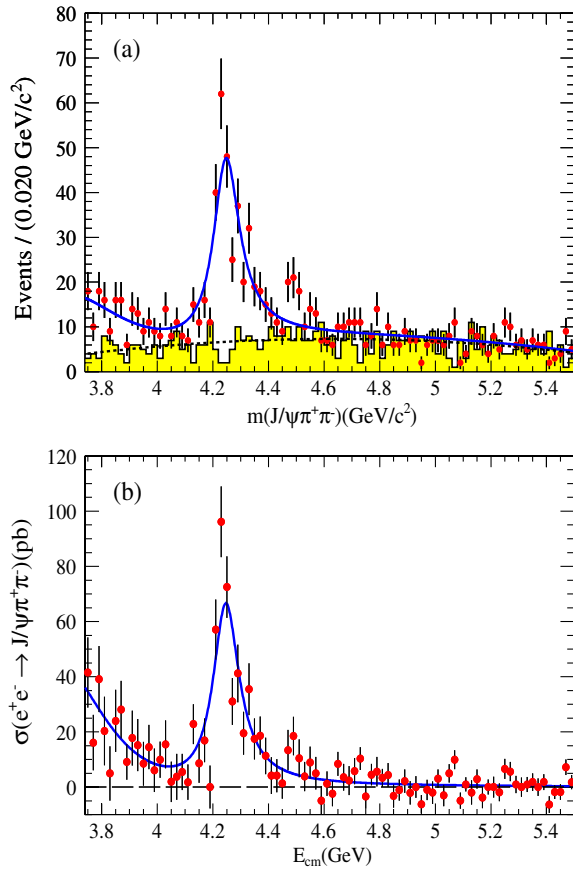


FIG. 2 (color online). (a) The $J/\psi \pi^+ \pi^-$ mass spectrum from $3.74 \text{ GeV}/c^2$ to $5.5 \text{ GeV}/c^2$; the points represent the data and the shaded histogram is the background from the J/ψ sidebands; the solid curve represents the fit result, and the dashed curve results from the simultaneous fit to the background; (b) the measured $e^+ e^- \rightarrow J/\psi \pi^+ \pi^-$ cross section as a function of c.m. energy; the solid curve results from the fit shown in (a).

production of the $Y(4260)$, and beyond $\sim 4.8 \text{ GeV}/c^2$ the data are consistent with background only. There is a small excess of events near $4.5 \text{ GeV}/c^2$, which we choose to attribute to statistical fluctuation. In this regard, we note that no corresponding excess is observed in Ref. [14]. The background contribution is featureless throughout the mass region being considered.

In order to extract the parameter values of the $Y(4260)$, we perform an unbinned, extended-maximum-likelihood fit in the region $3.74\text{--}5.5 \text{ GeV}/c^2$ to the $J/\psi \pi^+ \pi^-$ distribution from the J/ψ signal region, and simultaneously to the background distribution from the J/ψ sidebands. The background is fitted using a third-order polynomial in $J/\psi \pi^+ \pi^-$ mass, m . The mass-dependence of the signal function is given by $f(m) = \epsilon(m) \cdot \mathcal{L}(m) \cdot \sigma(m)$, where $\epsilon(m)$ is the mass-dependent signal-selection efficiency from MC simulation with a $J/\psi \pi^+ \pi^-$ phase space distribution, and $\mathcal{L}(m)$ is the mass-distributed luminosity [23], where we ignore the small corrections due to initial-state emission of additional soft photons; $\epsilon(m)$ increases from

9.5% at $3.74 \text{ GeV}/c^2$ to 15.5% at $5.5 \text{ GeV}/c^2$, and $\mathcal{L}(m)$ from $35 \text{ pb}^{-1}/20 \text{ MeV}$ to $61.3 \text{ pb}^{-1}/20 \text{ MeV}$ over the same range. The cross section, $\sigma(m)$, is given by the incoherent sum $\sigma(m) = \sigma_{\text{NY}}(m) + \sigma_{\text{BW}}(m)$, where we choose $\sigma_{\text{NY}}(m)$ to be a simple exponential function. This provides an adequate description of the low-statistics non- $Y(4260)$ (NY) contributions, and approaches zero from above at mass $\sim 4.8 \text{ GeV}/c^2$ (see Fig. 2). The function $\sigma_{\text{BW}}(m)$ represents the cross section for the production of the $Y(4260)$, and is given by

$$\sigma_{\text{BW}}(m) = \frac{12\pi C}{m^2} \cdot \frac{PS(m)}{PS(m_Y)} \cdot \frac{\Gamma_{e^+e^-} \cdot \mathcal{B}(J/\psi \pi^+ \pi^-) \cdot m_Y^2 \cdot \Gamma_Y}{(m_Y^2 - m^2)^2 + m_Y^2 \Gamma_Y^2}, \quad (1)$$

where m_Y and Γ_Y are the mass and width of the $Y(4260)$, $\Gamma_{e^+e^-}$ is the partial width for $Y(4260) \rightarrow e^+ e^-$, $\mathcal{B}(J/\psi \pi^+ \pi^-)$ is the branching fraction for $Y(4260) \rightarrow J/\psi \pi^+ \pi^-$, and $C = 0.3894 \times 10^9 \text{ GeV}^2 \text{ pb}$. The function $PS(m)$ represents the mass dependence of $J/\psi \pi^+ \pi^-$ phase space, and $PS(m_Y)$ is its value at the mass of the $Y(4260)$. In the likelihood function, $\sigma_{\text{BW}}(m)$ is multiplied by $\mathcal{B}(J/\psi \rightarrow l^+ l^-)$, the branching fraction sum of the $e^+ e^-$ and $\mu^+ \mu^-$ decay modes [18], since the fit is to the observed events. In the fit procedure $f(m)$ is convolved with a Gaussian resolution function obtained from MC simulation. This function has a r.m.s. deviation which increases linearly from $2.1 \text{ MeV}/c^2$ at $\sim 3.5 \text{ GeV}/c^2$ to $5 \text{ MeV}/c^2$ at $\sim 4.3 \text{ GeV}/c^2$. The results of the fit are shown in Fig. 2(a). The parameter values obtained for the $Y(4260)$ are $m_Y = 4245 \pm 5(\text{stat}) \text{ MeV}/c^2$, $\Gamma_Y = 114^{+16}_{-15}(\text{stat}) \text{ MeV}$, and $\Gamma_{e^+e^-} \times \mathcal{B}(J/\psi \pi^+ \pi^-) = 9.2 \pm 0.8(\text{stat}) \text{ eV}$.

For each $J/\psi \pi^+ \pi^-$ mass interval, i , we calculate the $e^+ e^- \rightarrow J/\psi \pi^+ \pi^-$ cross section after background subtraction using

$$\sigma_i = \frac{n_i^{\text{obs}} - n_i^{\text{bkg}}}{\epsilon_i \cdot \mathcal{L}_i \cdot \mathcal{B}(J/\psi \rightarrow l^+ l^-)}, \quad (2)$$

with n_i^{obs} and n_i^{bkg} the number of observed and background events, respectively, for this interval; ϵ_i , and \mathcal{L}_i are the values of $\epsilon(m)$ and $\mathcal{L}(m)$ [23] at the center of interval i .

The resulting cross section is shown in Fig. 2(b), where the solid curve is obtained from the simultaneous likelihood fit. The corresponding estimates of systematic uncertainty are due to luminosity (1%), tracking (5.1%), $\mathcal{B}(J/\psi \rightarrow l^+ l^-)$ (0.7%), efficiency (1%) and PID (1%); combined in quadrature. These yield a net systematic uncertainty of 5.4%, as indicated in Table I.

The reaction $e^+ e^- \rightarrow J/\psi \pi^+ \pi^-$ has been studied at the c.m. energy of the $\psi(3770)$ by the CLEO [24] and BES [25] collaborations. The former reported the value $12.1 \pm 2.2 \text{ pb}$ for the $e^+ e^- \rightarrow \psi(3770) \rightarrow J/\psi \pi^+ \pi^-$ cross section, after subtraction of the contribution resulting from radiative return to the $\psi(2S)$. The dependence on E_{cm} of our fitted cross section, shown by the curve in Fig. 2(b),

STUDY OF THE REACTION ...

TABLE I. Systematic uncertainty estimates for the $Y(4260)$ parameter values.

Source	$\Gamma_{e^+e^-} \cdot \mathcal{B}(\%)$	Mass (MeV/ c^2)	Γ (MeV)
Fit procedure	+1.5 -0.5	+0 -1	+2 -1
Mass Scale	...	± 0.6	...
Mass resolution	± 1.5
MC dipion model	± 3.6
Decay angular momentum	± 3.6	± 3.5	± 7
Luminosity, etc. (see text)	± 5.4

yields the value $31 \pm 5(\text{stat}) \pm 2(\text{syst})$ pb at the $\psi(3770)$ with no subtraction of a $\psi(2S)$ contribution. This is compatible with the much more precise CLEO result obtained after subtraction. No cross section value is reported in Ref. [25], but the results of the BES analysis agree within their significantly larger uncertainties with those from CLEO.

The systematic uncertainties on the measured values of the $Y(4260)$ parameters include contributions from the fitting procedure (evaluated by changing the fit range and the background parametrization), the uncertainty in the mass scale resulting from the uncertainties associated with the magnetic field and with our energy-loss correction procedures, the mass-resolution function, and the change in efficiency when the dipion distribution is simulated using the solid histogram in Fig. 3(c), which is described below. In Eq. (1) it is assumed that $Y(4260)$ decay to a J/ψ and a scalar dipion occurs in an S -wave orbital angular momentum state. However, a D -wave decay between the J/ψ and the $\pi^+\pi^-$ system can occur also, and for this hypothesis the fitted central values of mass, width, and $\Gamma_{e^+e^-} \times \mathcal{B}(J/\psi \pi^+\pi^-)$ become 4237 MeV/ c^2 , 100 MeV, and 8.5 eV, respectively. We assign half the change in central value of each quantity as a conservative estimate of systematic uncertainty associated with the decay angular momentum. Uncertainties associated with luminosity, tracking, $\mathcal{B}(J/\psi \rightarrow l^+l^-)$, efficiency and PID affect only $\Gamma_{e^+e^-} \cdot \mathcal{B}$, and their net contribution is 5.4%, as we discussed previously. Our estimates of systematic uncertainty are summarized in Table I, and are combined in quadrature to obtain the values which we quote for the $Y(4260)$. We also increase the fitted mass value of the $Y(4260)$ to 4245 MeV/ c^2 to reflect the mass shift which we observe for the $\psi(2S)$.

We now consider the $\pi^+\pi^-$ system from $Y(4260)$ decay to $J/\psi \pi^+\pi^-$. Since the $Y(4260)$ has $I(J^{PC}) = 0(1^{--})$ and its width indicates strong decay, the $\pi^+\pi^-$ system has $I(J^{PC}) = 0(0^{++})$ or $I(J^{PC}) = 0(2^{++})$. For the region $4.15 \leq m(J/\psi \pi^+\pi^-) \leq 4.45$ GeV/ c^2 , the $\pi^+\pi^-$ mass distribution after subtraction of that from the J/ψ sideband regions is shown in Fig. 3(a). The region below 0.32 GeV/ c^2 is excluded since it is severely depopulated by the procedure used to remove e^+e^- pair contamination. The distribution decreases from threshold to near zero at ~ 0.6 GeV/ c^2 , rises steadily to a maximum at

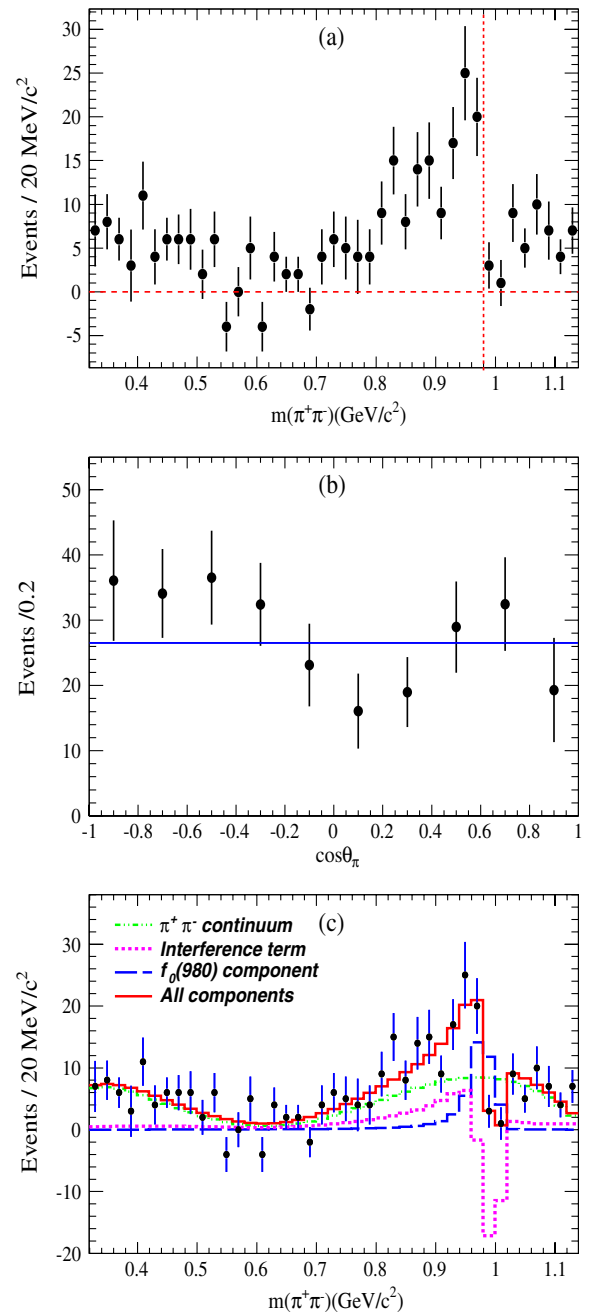


FIG. 3 (color online). (a) The background-subtracted $\pi^+\pi^-$ mass distribution for the $Y(4260)$ signal region; the dashed vertical line is at the nominal $f_0(980)$ mass value [18]; (b) the corresponding $\cos\theta_\pi$ distribution; the fitted line is for an S -wave description; (c) the result of the fit using the model of Eq. (3).

~ 0.95 GeV/ c^2 , decreases rapidly to near zero again at ~ 1 GeV/ c^2 , and increases thereafter. The distribution is consistent with previous measurements [6,14].

We define θ_π as the angle between the π^+ direction and that of the recoil J/ψ , both in the dipion rest frame. The distribution in $\cos\theta_\pi$ is shown in Fig. 3(b). The fitted line represents S -wave decay, and provides an adequate

description of the data ($\chi^2/\text{NDF} = 12.3/9$, probability = 19.7%); there is no need for a D -wave contribution, e.g., from $f_2(1270) \rightarrow \pi^+ \pi^-$ decay.

The mass distribution near 1 GeV/ c^2 suggests coherent addition of a nonresonant $\pi^+ \pi^-$ amplitude and a resonant amplitude describing the $f_0(980)$. If the peak near 950 MeV/ c^2 is attributed to a nonresonant amplitude with phase near 90° , the coherent addition of the resonant $f_0(980)$ amplitude, in the context of elastic unitarity, could result in the observed behavior, which is similar to that of the $I = 0 \pi^+ \pi^-$ elastic scattering cross section near 1 GeV (Fig. 2, p. VII.38, of Ref. [26]). However, we have no phase information with which to support this conjecture.

The distribution in Fig. 3(a) for $m_{\pi\pi} < 0.9$ GeV/ c^2 is qualitatively similar to that observed for the decay $Y(3S) \rightarrow Y(1S)\pi^+ \pi^-$ [27]. There, the dipion mass distribution decreases from a maximum near threshold to a significantly nonzero minimum at $\sim 0.6\text{--}0.7$ GeV/ c^2 , before rising steeply toward 0.8 GeV/ c^2 before being cut off by the kinematic limit (0.895 GeV/ c^2). The CLEO data are well-described in terms of a QCD multipole expansion [28,29] up to $m_{\pi\pi} \sim 0.7$ GeV/ c^2 , but the sharp rise thereafter is not well-accommodated. This shortcoming is more readily apparent for the much larger *BABAR* data sample for this same process [30]. There the distribution begins a rapid rise toward the $f_0(980)$ region, as in Fig. 3(a), but turns over at ~ 0.85 because of the kinematic limit at 0.895 GeV/ c^2 . The CLEO multipole expansion fit involves two amplitudes whose relative phase ($\pm 155^\circ$) causes destructive interference, and hence the minimum in the mass distribution at $\sim 0.6\text{--}0.7$ GeV/ c^2 . The amplitudes are of similar magnitude in this region, and so a relative phase of $\pm 180^\circ$ could yield near-zero intensity, as observed in Fig. 3(a). This phase value would result in an approximately real amplitude. However it would contain no explicit $f_0(980)$ contribution, which seems necessary to a description of the data of Fig. 3(a), and so we attempt to describe the entire distribution using the following simple model.

The nonresonant intensity distribution requires three turning points, as in the CLEO multipole expansion description, and so we choose to represent it by a fourth-order polynomial, $T(m_{\pi\pi})$, where $m_{\pi\pi}$ is the invariant mass of the $\pi^+ \pi^-$ system. From the phase requirement discussed above, it follows that the corresponding amplitude can be chosen to be real and represented by $\sqrt{T(m_{\pi\pi})}$. To this amplitude we add the complex S -wave $\pi^+ \pi^-$ amplitude obtained from the *BABAR* analysis of $D_s^+ \rightarrow \pi^+ \pi^- \pi^+$

decay [31], which shows clear resonant behavior at the $f_0(980)$. We perform a χ^2 -fit to the data of Fig. 3(a) using

$$f(m_{\pi\pi}) = \left| \sqrt{T(m_{\pi\pi})} + e^{i\phi} F_{f_0(980)}(m_{\pi\pi}) \right|^2 \cdot p \cdot q, \quad (3)$$

where $F_{f_0(980)}$ is proportional to the complex $\pi^+ \pi^-$ amplitude of Ref. [31], and the phase ϕ is determined by the fit; p is the π^+ momentum in the $\pi^+ \pi^-$ rest frame, and q is the J/ψ momentum in the $J/\psi \pi^+ \pi^-$ rest frame. We use the fitted $Y(4260)$ mass value in calculating q , which implies a kinematic limit of 1.15 GeV/ c^2 for the fit function. The result is shown in Fig. 3(c). The fit is good ($\chi^2/\text{NDF} = 33.6/35$, probability = 53.6%), and the interference contribution is important for the description of the region near 1 GeV/ c^2 ($\phi = 28^\circ \pm 24^\circ$). The $f_0(980)$ amplitude squared gives 0.17 ± 0.13 (stat) for the branching ratio $\mathcal{B}(J/\psi f_0(980), f_0(980) \rightarrow \pi^+ \pi^-) / \mathcal{B}(J/\psi \pi^+ \pi^-)$. This is somewhat smaller than the prediction of Ref. [32], where it is proposed that the $f_0(980)$ contribution should be dominant.

In summary, we have used ISR events to study the process $e^+ e^- \rightarrow J/\psi \pi^+ \pi^-$ in the c.m. energy range 3.74–5.50 GeV. For the $Y(4260)$ we obtain $m_Y = 4245 \pm 5(\text{stat}) \pm 4(\text{syst})$ MeV/ c^2 , $\Gamma_Y = 114_{-15}^{+16}(\text{stat}) \pm 7(\text{syst})$ MeV, and $\Gamma_{e^+ e^-} \times \mathcal{B}(J/\psi \pi^+ \pi^-) = 9.2 \pm 0.8(\text{stat}) \pm 0.7(\text{syst})$ eV. These results represent an improvement in statistical precision of $\sim 30\%$ over the previous *BABAR* results [6], and agree very well in magnitude and statistical precision with the results of the Belle fit which uses a single Breit-Wigner resonance to describe the data [14]. We do not confirm the broad enhancement at 4.01 GeV/ c^2 reported in Ref. [14]. The dipion system for the $Y(4260)$ decay is in a predominantly S -wave state. The mass distribution exhibits an $f_0(980)$ signal, for which a simple model indicates a branching ratio with respect to $J/\psi 2\pi^+ \pi^-$ of 0.17 ± 0.13 (stat).

We are grateful for the excellent luminosity and machine conditions provided by our PEP-II colleagues, and for the substantial dedicated effort from the computing organizations that support *BABAR*. The collaborating institutions wish to thank SLAC for its support and kind hospitality. This work is supported by DOE and NSF (USA), NSERC (Canada), CEA and CNRS-IN2P3 (France), BMBF and DFG (Germany), INFN (Italy), FOM (The Netherlands), NFR (Norway), MES (Russia), MICIIN (Spain), STFC (United Kingdom). Individuals have received support from the Marie Curie EIF (European Union) and the A. P. Sloan Foundation (USA).

- [1] S. K. Choi *et al.*, *Phys. Rev. Lett.* **91**, 262001 (2003).
 [2] S. Uehara *et al.*, *Phys. Rev. Lett.* **96**, 082003 (2006).
 [3] S. K. Choi *et al.*, *Phys. Rev. Lett.* **94**, 182002 (2005).

- [4] K. Abe *et al.*, *Phys. Rev. Lett.* **98**, 082001 (2007).
 [5] T. Appelquist, R. M. Barnett, and K. D. Lane, *Annu. Rev. Nucl. Part. Sci.* **28**, 387 (1978).

- [6] B. Aubert *et al.*, *Phys. Rev. Lett.* **95**, 142001 (2005).
- [7] T.E. Coan *et al.* *Phys. Rev. Lett.* **96**, 162003 (2006).
- [8] B. Aubert *et al.*, *Phys. Rev. D* **76**, 111105 (2007); **79**, 092001 (2009); G. Pakhlova *et al.*, *Phys. Rev. Lett.* **98**, 092001 (2007); *Phys. Rev. D* **77**, 011103 (2008).
- [9] P. del Amo Sanchez *et al.*, *Phys. Rev. D* **82**, 052004 (2010); J. Libby *et al.*, *Nucl. Phys. B, Proc. Suppl.* **181–182**, 127 (2008).
- [10] I. Bigi *et al.*, *Phys. Rev. D* **72**, 114016 (2005).
- [11] L. Maiani *et al.*, *Phys. Rev. D* **72**, 031502 (2005).
- [12] C. -F. Qiao, *J. Phys. G* **35**, 075008 (2008).
- [13] S. -L. Zhu, *Phys. Lett. B* **625**, 212 (2005).
- [14] C.Z. Yuan *et al.*, *Phys. Rev. Lett.* **99**, 182004 (2007).
- [15] B. Aubert *et al.*, *Phys. Rev. Lett.* **98**, 212001 (2007).
- [16] X.L. Wang *et al.*, *Phys. Rev. Lett.* **99**, 142002 (2007).
- [17] B. Aubert *et al.*, *Nucl. Instrum. Methods Phys. Res., Sect. A* **479**, 1 (2002); W. Menges, *IEEE Nucl. Sci. Symp. Conf. Rec.* **5**, 1470 (2006).
- [18] K. Nakamura *et al.*, *J. Phys. G* **37**, 075021 (2010), and partial update for the 2012 edition (<http://pdg.lbl.gov>).
- [19] G. Bonneau and F. Martin, *Nucl. Phys.* **B27**, 381 (1971); H.Czyz *et al.*, *Eur. Phys. J. C* **18**, 497 (2001); D.J. Lange, *Nucl. Instrum. Methods Phys. Res., Sect. A* **462**, 152 (2001).
- [20] S. Agostinelli *et al.*, *Nucl. Instrum. Methods Phys. Res., Sect. A* **506**, 250 (2003).
- [21] B. Aubert *et al.*, *Phys. Rev. D* **80**, 092005 (2009).
- [22] B. Aubert *et al.*, *Phys. Rev. D* **72**, 052006 (2005).
- [23] E. A. Kuraev and V. S. Fadin, *Sov. J. Nucl. Phys.* **41**, 466 (1985).
- [24] N.E. Adam *et al.* , *Phys. Rev. Lett.* **96**, 082004 (2006).
- [25] J.Z. Bai *et al.*, *Phys. Lett. B* **605**, 63 (2005).
- [26] K. Hikasa *et al.* *Phys. Rev. D* **45**, Part II (1992).
- [27] D. Cronin-Hennessy *et al.* *Phys. Rev. D* **76**, 072001 (2007).
- [28] L. S. Brown and R. N. Cahn, *Phys. Rev. Lett.* **35**, 1 (1975).
- [29] T. -M. Yan, *Phys. Rev. D* **22**, 1652 (1980).
- [30] E. Guido, Ph.D. thesis, Università degli Studi di Genova, 2011 (*BABAR Publications*, THESIS-12/003, 2012);
- [31] B. Aubert *et al.*, *Phys. Rev. D* **79**, 032003 (2009).
- [32] A. Martinez Torres *et al.*, *Phys. Rev. D* **80**, 094012 (2009).